ELSEVIER

Molecular architecture–mechanical behaviour relationships in epoxy networks

O. Sindt and J. Perez*
Groupe d'Etudes de Métallurgie Physique et de Physique des Matériaux, Bât. 502, Insa Lyon, 69621 Villeurbanne Cedex, France

and J. F. Gerard
Laboratoire des Matériaux Macromoléculaires et Composites, Bât. 303, Insa Lyon, 69621 Villeurbanne Cedex, France
(Received 10 March 1995)

The mechanical properties of various epoxy–amine networks were studied as a function of the flexibility of the polymer chains and the crosslink density. Physical characterization and low-frequency dynamic mechanical spectroscopy gave insight into the structure. Compression test properties were correlated to the molecular arrangements, and then low- and high-stress properties were analysed with a unique theory leading to relationships between the thermomechanical test results and the molecular architecture of these networks. Copyright © 1996 Elsevier Science Ltd.

(Keywords: epoxy; mechanical behaviour; molecular mobility; molecular architecture)

INTRODUCTION

Epoxy resins are now widely used in industrial applications such as adhesives and matrices for composite materials. High performances need to be achieved through the synthesis and processing of the materials; especially, a good mechanical behaviour (stiffness and toughness) is expected. That is why a better understanding of the structure–processing–properties relationships is required. In the past decades, numerous papers have been devoted to this subject, especially in the case of epoxy–amine networks. In fact, the chemistry of these epoxy systems is well known; thus, they could be good models for a generalized description of the molecular architecture–mechanical properties relationships of polymer networks. By means of this approach, in a final step, the structure could be tailored to the desired final properties.

The molecular architecture can be modified in different ways by changing the crosslink density and/or the flexibility of chains between crosslinks. The crosslink density can be varied by changing the stoichiometric ratio and the extent of cure[1-4]. In this case, the soluble fractions and/or the dangling chains alter the network topology and the conclusions are not clear. A second way of modifying the crosslink density consists of changing the molar mass of the epoxy comonomer[5,6], although a distribution of molar mass between crosslinks is also introduced. A better method is to control the crosslink density by using a mixture of monoamines and primary diamines[7-9].

The other important characteristic of the network architecture is the flexibility of the chains between the crosslinks. This can be changed by the use of aliphatic epoxy prepolymers instead of the usual aromatic epoxy monomers[10,11]. Moreover, the nature of the amine comonomer can be changed[12,13].

The aim of this work is to study the influence of both of these parameters (crosslink density and flexibility of the chains between crosslinks) on the thermomechanical properties. Two main domains will be explored: (a) small-deformation range, by means of low-frequency spectroscopy (isochronal conditions); and (b) high-deformation range, by means of compression tests. Then, we propose to model the results with a theory allowing us to establish relationships between the macroscopic mechanical behaviour and molecular architecture.
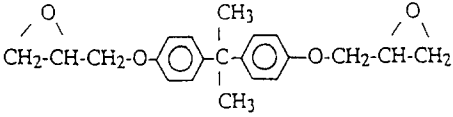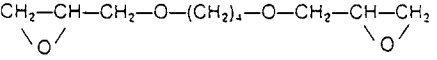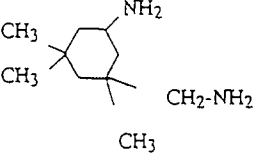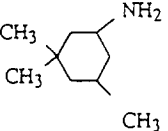
MATERIALS

The epoxy networks were synthesized from the reaction between an epoxy prepolymer (difunctional) and a primary amine conomomer (tetrafunctional). These reagents are described in *Table 1*. The reaction was carried out in bulk with a stoichiometric ratio (amino hydrogen to epoxy = 1) after degassing at 60°C for 30 min under vacuum. The reactive system was cured using a cure schedule chosen in order to obtain a maximum glass transition temperature[14].

The reference network was based on the diglycidyl ether of bisphenol A epoxy prepolymer (DGEBA) and a cycloaliphatic diamine, 5-amino-1,3,3-trimethylcyclohexylamine (isophorone diamine, denoted IPD). In order to change the flexibility of the macromolecular chains between crosslinks, the DGEBA prepolymer was replaced by an aliphatic diepoxy monomer, the diglycidyl

---

*To whom correspondence should be addressed

Table 1 Reagents used to synthesize the epoxy networks

Reagent	Formula	Supplier
Diglycidyl ether of bisphenol A (DGEBA)		Dow Chemicals (DER 332)
	$n = 0.03$	
Diglycidyl ether of 1,4-butanediol (DGEBD)		Aldrich
Isophorone diamine (IPD)		Huls
Trimethylcyclohexylamine (TMCA)		Veba Chem

ether of 1,4-butanediol (DGEBD). The change of the crosslink density was achieved by introducing a difunctional primary amine comonomer, 1,3,3-trimethylcyclohexylamine (TMCA), acting as a chain extender. The molecular structure of this amine is similar to that of IPD in order to avoid a change in the nature of the chains between crosslinks. In the DGEBA/IPD/TMCA network considered, 50% of the amino hydrogen groups belong to the monoamine TMCA, keeping the stoichiometric ratio equal to 1 (see *Table 1*).

Owing to the high vapour pressure of the amines, the cure schedule adopted for the DGEBA/IPD and DGEBA/IPD/TMCA reactive systems consists of a heating from room temperature up to 140°C (2°C min^{-1}), 1 h at 140°C, a second heating from 140°C up to 190°C (2°C min^{-1}) and a final stay at 190°C for 6 h. For the DGEBD/IPD reactive system, the cure schedule consists of 1 h at 100°C followed by 10 h at 190°C. The same heating rate (2°C min^{-1}) between steps was selected. The materials were moulded into 6 mm thick plates and 8 mm diameter cylinders.

TECHNIQUES

Calorimetric measurements and physical characterization

The glass transition temperature T_g (onset and ΔT_g) and the change in the heat capacity ΔC_p were recorded using differential scanning calorimetry (d.s.c.) with a Mettler TA3000 apparatus (heating rate 7.5°C min^{-1}).

The thermal expansion coefficients in both glassy and rubbery states, α_{glass} and α_{rub} respectively, were determined using a Perkin Elmer TMA7 thermomechanical analyser (heating rate 5°C min^{-1}) on cuboidal specimens $(2 \times 5 \times 5 \text{ mm}^3)$. The volume expansion coefficients were derived from the linear ones.

Densities at room temperature were determined by Archimedes' method.

Low-frequency dynamic mechanical spectroscopy (d.m.s.)

A spectrometer developed in our laboratory[15] and provided by Metravib was used. The temperature range

was from 90 to 700 K and the frequency range was from 10^{-5} to 1 Hz. This spectrometer worked in torsion; thus, we obtained the dynamic shear modulus G^* $(=G' + iG'')$ and $\tan \phi$ $(=G''/G')$, where G' is the storage modulus, G'' is the loss modulus and $\tan \phi$ characterizes the internal friction.

Ultrasonic (u.s.) measurements

This technique leads to the determination of the unrelaxed elastic constants of the materials. Tests were performed at different frequencies (1, 2.25, 5 and 10 MHz) with two kinds of sensors: longitudinal and transverse waves in emission–reception conditions (i.e. the same sensor was the emitter and the receiver). If V_L and V_T are the longitudinal and the tranverse velocity, respectively, of the u.s. waves, the shear modulus G_{us}, the bulk modulus B_{us} and the Young's modulus E_{us} are defined as:

$$G_{us} = \rho V_T^2$$

$$B_{us} = \rho V_T^2 \left(\frac{V_L^2}{V_T^2} - \frac{4}{3} \right)$$

$$E_{us} = \rho V_T^2 \left(\frac{3V_L^2 - 4V_T^2}{V_L^2 - V_T^2} \right)$$

Compression tests

These tests have been performed on an Adamel Lhomargy compression machine. The testing temperature could be set between -130 and $+50$°C and the crosshead speed could vary between 10^{-2} and 45×10^{-2} mm min^{-1} (15×10^{-2} mm min^{-1} was selected in the present study).

The considered specimens were cylinders (8 mm diameter, 10 mm long). The deformation rate was kept constant until the plastic consolidation domain was reached. At this time, the crosshead was stopped and

stress relaxation was measured (i.e. stress vs. time). The apparent activation volume V_{exp} was deduced by applying Guiu and Pratt's[16] equation:

$$\sigma(t) - \sigma(0) = \frac{kT}{V_{\text{exp}}} \ln\left(1 + \frac{t}{t_{\text{p}}}\right)$$

Other deformation rates have also been checked in order to study the influence of this parameter.

GENERAL CHARACTERIZATION OF THE MATERIALS

The characteristics of the epoxy networks considered here are reported in *Table 2*. As expected, as the TMCA is added as a chain extender, the crosslink decreases because the molar mass between crosslinks $\bar{M}_{\text{C}}$ increases. For the stoichiometric ratio equal to 1, $\bar{M}_{\text{C}}$ is computed from the molar mass and the amount of each monomer as follows:

$$\bar{M}_{\text{C}} = \frac{[N_{\text{TMCA}}M_{\text{TMCA}} + N_{\text{IPD}}M_{\text{IPD}} + (N_{\text{TMCA}} + 2M_{\text{IPD}})]M_{\text{E}}}{3M_{\text{IPD}}}$$

where N_{TMCA} and N_{IPD} are the number of moles from TMCA and IPD respectively; M_{TMCA} and M_{IPD} are the molar mass of TMCA and IPD, respectively; and $\bar{M}_{\text{E}}$ is the average molar mass of the epoxy prepolymer. As a consequence, the glass transition temperature T_{g} of the epoxy network based only on the IPD hardener is higher than that of the DGEBA/IPD/TMCA network.

The substitution of an aromatic epoxy prepolymer by an aliphatic one (DGEBD) induces a large decrease of T_{g}, owing to the fact that the DGEBD chains between crosslinks are more flexible. However, this substitution induces not only a change in the flexibility but also a slight increase of the crosslink density (*Table 2*). The molecular masses between crosslinks for the DGEBD/IPD and DGEBD/IPD are not similar[10,17] (*Table 2*).

The changes in crosslink density or flexibility induce slight changes in the thermal expansion coefficient in the glassy state, α_{glass}, whereas a large effect is observed on α_{rub}, i.e. in the rubbery state, so that the difference $\Delta\alpha$ is very dependent on these structural changes.

The moduli at high frequency have also been measured

with ultrasonic waves. The aim of such measurements is to determine the unrelaxed shear modulus (G), which would only differ slightly from the 0 K modulus (G_0) due to the phonon effect. Different frequencies have been checked until the dependence of G with frequency was negligible. Finally, measurements have been performed at 10 MHz. We have verified that, for that frequency, the unrelaxed shear modulus is measured referring to the mechanical relaxation observed at lower temperature in spectra obtained at 1 Hz (γ relaxation). The results are given in *Table 2*. It is clear that increasing flexibility or decreasing crosslink density have the same effect on the different moduli: E (Young's modulus) and G (shear modulus) are lower because the macromolecular solid has weaker van der Waals intermolecular interactions, i.e. a lower cohesion, since the modulus is proportional to the second derivative of the interaction energy[18].

However, if the B/G ratio is taken into account, the effect of flexibility is not displayed, whereas the crosslink density has a great influence. As the crosslink density increases, this ratio decreases. In other words, with the introduction of crosslinks, the bonding effect in the system changes from van der Waals undirected forces (or central forces) to more directed forces, i.e. with a higher covalent bonding effect[19].

THERMOMECHANICAL BEHAVIOUR

Results of dynamic mechanical spectroscopy

The dynamic mechanical spectra of the epoxy networks at 1 Hz given in *Figures 1a* and *1b* display two relaxation zones. In each case, G' decreases sharply in the high-temperature range where the loss factor (i.e. $\tan\phi$) displays a maximum. This main relaxation phenomenon, denoted α, is due to generalized macromolecular chain movements. Thus, α is associated to the glass transition of the polymer.

The low-temperature $\tan\phi$ peak characterizes the secondary relaxation, denoted β (near 220 K at 1 Hz) (*Figures 1a* and *1b*). This one is associated to the motions of hydroxy ether groups[20–22]. A smaller decrease in G' is observed in relation with this relaxation,

In the case of the more flexible network, i.e. DGEBD/IPD, a third relaxation, denoted γ, is evidenced at low

Table 2 Physicochemical properties of the three networks

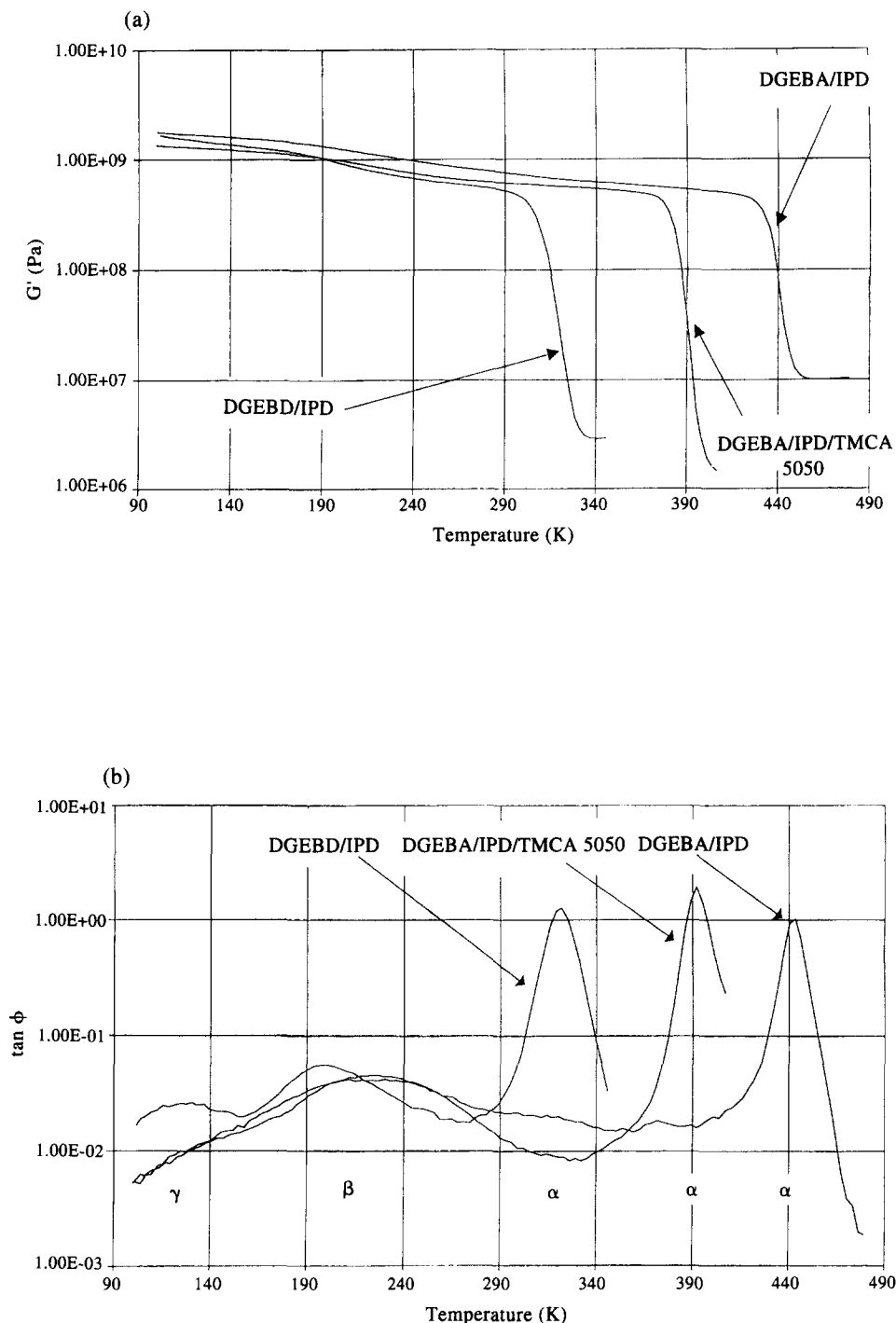|	DGEBA/IPD	DGEBA/IPD/TMCA 50/50	DGEBD/IPD
T_{g} (K)	436	383	326
ΔT_{g} (K) (calorimetry)	9	13	11
T_{g} (K) (dilatometry)	436	393	329
ΔC_{p} ($\text{J g}^{-1}\text{K}^{-1}$)	0.26	0.40	0.33
Density (kg m^{-3})	1131	1112	1122
α_{glass} ($10^{-4}\,\text{K}^{-1}$)	2.46	2.83	2.99
$\Delta\alpha$ ($10^{-4}\,\text{K}^{-1}$)	3.50	5.82	6.40
E (GPa)	4.71	4.49	4.15
B (GPa)	5.01	5.25	5.80
G (GPa)	1.75	1.65	1.33
B/G	2.86	3.18	4.35
$\bar{M}_{\text{C}}$ (kg)	0.383	1.255	0.454
(mol kg^{-1})	2.35	1.10	3.50

Figure 1 Plots of (a) G' (log scale) and (b) $\tan\phi$ (log scale) vs. temperature at 1 Hz

temperatures and is due to the motions of the methylene units (near 130 K at 1 Hz)[7].

From dynamic mechanical spectra at various frequencies, it is possible to determine the apparent activation energies of the secondary processes, β and γ, occurring in the glassy state from an Arrhenius law:

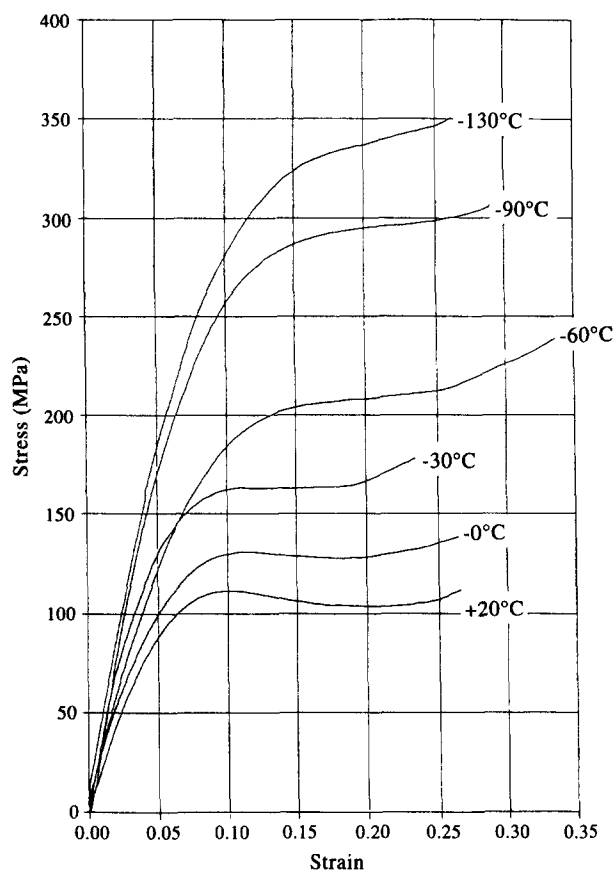$$f = A \exp\left(-\frac{E_a^{\ddagger}}{RT}\right)$$

The calculated apparent activation energies of these β and γ relaxations are denoted $E_{a\beta}^{\ddagger}$ and $E_{a\gamma}^{\ddagger}$, respectively. As reported in *Table 3*, the change of flexibility of the chains between crosslinks has no effect on $E_{a\beta}^{\ddagger}$, in

contrast to the crosslink density. This effect was also observed in other structural series[8] and could be attributed to the existence of stronger van der Waals interactions in the less crosslinked networks[23]. In addition, the values of $E_{a\beta}^{\ddagger}$ are close to those reported by Won[8] and Urbacewski[10] for DGEBA/IPD and DGEBD/4,4'-diamino-3,3'-dimethyldicyclohexylmethane, respectively.

As reported by Charlesworth[7], only two constitutive methylene units in the diepoxide part are needed to induce a relaxation observed in the case of DGEBD/IPD network. This effect is due to the fact that the oxygen atoms can rotate in the same manner as the methylene. On the other hand, in an aliphatic amine comonomer,

Table 3 Activation energies of the secondary relaxations for the three networks

	$E_{a\beta}^{\ddagger}$ (kJ mol^{-1})	T_β (tan ϕ_{max}) at 1 Hz (K)	$E_{a\gamma}^{\ddagger}$ (kJ mol^{-1})	T_γ (tan ϕ_{max}) at 1 Hz (K)
DGEBA/IPD	54	222		
DGEBD/IPD	58	200	31	128
DGEBA/IPD/TMCA 50/50	70	227		

Figure 2 Effect of temperature on the stress–strain curves for DGEBA/IPD

Table 4 Plastic flow stress vs. temperature for the three networks

T (K)	σ_p (MPa)		
	DGEBA/IPD	DGEBD/IPD	DGEBA/IPD/TMCA 50/50
143	343.5	301	306
183	292	217	220
213	207	154	209
243	163		147.5
273	127		116.5
293	105.5	49	94
323	85	13	70
353			48

four methylene units are needed because of the fixed nitrogen atoms (crosslinks). The value of the apparent activation energy of the peak is also close to those reported[7,10]. The effects of the secondary relaxations on the Young's modulus at room temperature E_{RT} are described in the literature. In fact, as the crosslink density increases, E_{RT} decreases due to the highest amplitude of the peak for the highly crosslinked network. This phenomenon is called the 'antiplasticization effect'[8,9,23].

Mechanical tests at different temperatures

The aim of these compression tests is to study the influence of molecular features (crosslink density and flexibility of chains) on the plastic flow. Then, the effects of both temperature and deformation rate have been checked.

The evolution of the stress–strain curves for DGEBA/IPD shows three main domains (*Figure 2*): (i) a linear dependence of the stress vs. strain (elastic deformation), (ii) a maximum of stress, which is called yield stress (denoted σ_y), and (iii) a domain of nearly constant stress (this stress is the plastic flow stress, denoted σ_p), which

leads to plastic consolidation (increase of stress with strain).

The effect of temperature on the stress–strain curves is clearly shown in *Figure 2*: as the temperature increases, the plastic flow stress decreases. The same kind of effect was obtained for the two other networks, and the same evolution of σ_p vs. temperature was observed (*Table 4*). All of these results correspond to a deformation rate, dϵ/dt, equal to 2.4×10^{-4} s^{-1}.

At the beginning of the plastic consolidation domain, stress-relaxation (i.e. the evolution of stress with time at zero deformation rate) measurements have been done. Applying Guiu and Pratt's[16] equations, it was possible to determine the apparent activation volume V_{exp}. In order to compare this parameter with the sensitivity coefficient of stress *versus* strain rate:

$$V_{exp} = kT \frac{\partial \ln \dot{\epsilon}}{\partial \sigma}$$

different strain rates have been considered ($\dot{\epsilon} = 10^{-4}$, 2.5×10^{-4}, 4.5×10^{-4} and 7×10^{-4} s^{-1}). No differences have been observed between the two parameters and the same name (V_{exp}) will be used further. *Figure 3* gives V_{exp} as a function of reduced temperature T/T_g.

Analysis of results and relationships with molecular architecture

Epoxy resins, although inherently brittle materials, can undergo a large plastic deformation when they are submitted to high stresses. For low stresses, a linear viscoelastic behaviour related to the main relaxation is observed. In order to describe the response of the material to an applied stress, the earliest approaches were based upon viscoelastic models, using the Eyring theory of viscous flow. Later, physical descriptions of plastic flow of amorphous polymers at a molecular level were developed by Bowden[24] and Argon[25]. Yamini and Young[26] found that the plastic deformation of thermoset epoxy resins is similar to that of glassy thermoplastics. This observation has been confirmed by Oleinik[27], who proposed a qualitative description of the non-elastic deformation in terms of plastic shear transformation.
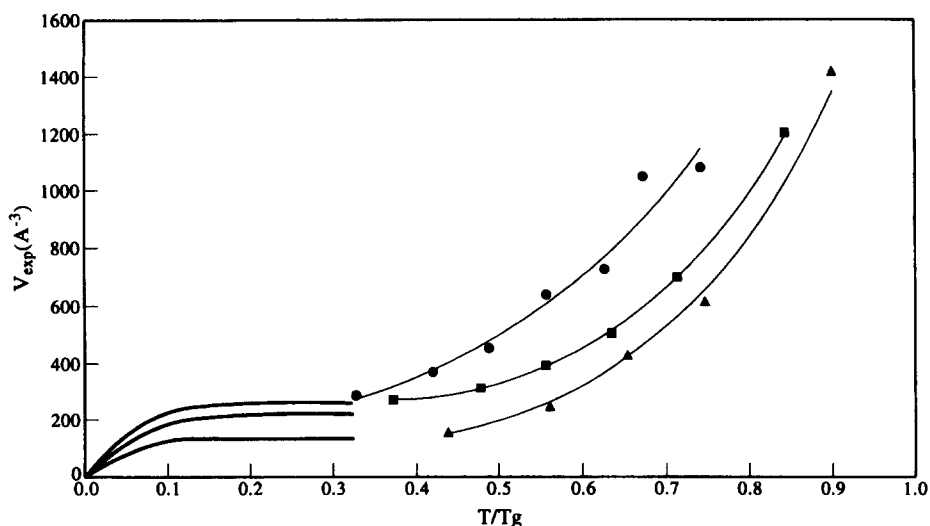
Figure 3 Effect of the normalized temperature, T/T_g, on the activation volume V_{exp}: symbols, experimental data for DGEBA/IPD/TMCA 50/50 (■), DGEBA/IPD (●) and DGEBD/IPD (▲); bold lines, calculated values from theoretical model; fine lines, mean evolution of V_{exp} with temperature

More quantitatively, the thermodynamic analysis of deformation, well known in the physical metallurgy field, was applied to amorphous polymers[28] and in particular to epoxy resins[29]. Actually, not one of these approaches offers relations that can be used for both low and high stresses (linear and non-linear stress–strain behaviour, respectively). Consequently, a new theory was developed; since it was presented in several papers previously published[30,31], only the three basic assumptions are recalled here:

(i) In amorphous condensed matter, nanofluctuations of density or quasi-point defects occur at a concentration C_d. C_d is temperature-dependent at T above T_g (metastable equilibrium), but is constant $C_d(T_g)$ at T below T_g when the microstructure is frozen in. It is worth while to note that negative nanofluctuations of density correspond to free volume; however, the quasi-point defect (q.p.d.) is a more general concept since it includes the possible occurrence of positive nanofluctuations of density, both fluctuations forming more disordered sites with less cohesive energy.

(ii) Based upon the concept of hierarchically correlated molecular motions, the mean time corresponding to a translational degree of freedom is given by:

$$\tau_{mol} = t_0 \left(\frac{\tau_1}{t_0}\right)^{1/\chi} \tag{1}$$

where t_0 is a scaling time and χ is a measure of how much hierarchically constrained are the correlated molecular entities during the deformation process. The value of χ is between 0 and 1: a zero value corresponds to a fully constrained situation with an infinite value for τ_{mol}, and a value of unit corresponds to a constraint-free situation with $\tau_{mol} = \tau_1$; then, χ increases with C_d. The time τ_1 corresponds to the time characteristic of the elementary molecular motion and was identified as the proper time of some secondary relaxations (e.g. β relaxation),
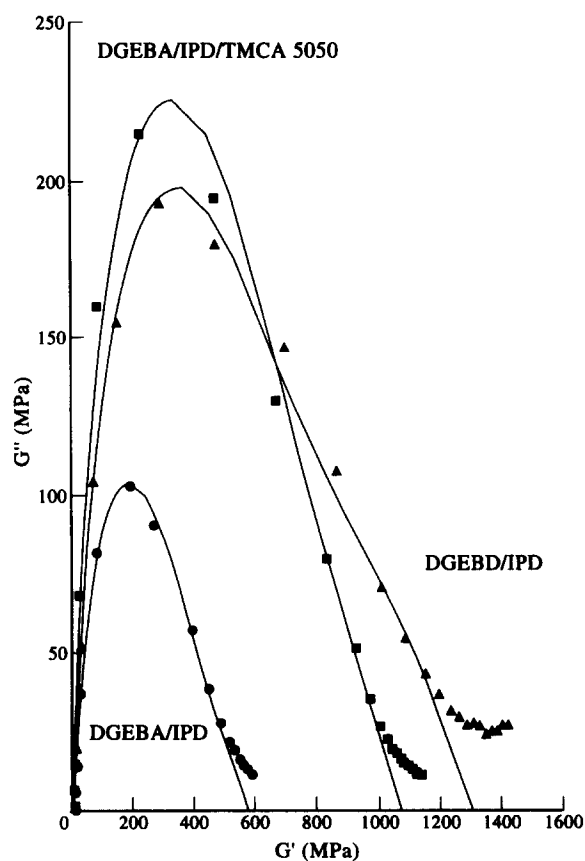
Figure 4 Cole–Cole representation for the three networks: symbols, experimental data for DGEBA/IPD/TMCA 50/50 (■); DGEBA/IPD (★) and DGEBD/IPD (●); lines, calculated from the model

so that:

$$\tau_1 = \tau_{1,0} \exp\left(\frac{U_1}{kT}\right) \tag{2}$$

(iii) The response to an applied stress was described in terms of thermomechanical nucleation, growth and then coalescence of shear microdomains, resulting in elastic and viscous deformation, respectively.

From these assumptions, the compliance was found to be given by:

$$J(t) = \frac{1}{G_u} + A\left\{1 - \exp\left[-\left(\frac{t}{\tau_{mol}}\right)^x\right]\right\}$$
$$+ A'\left(\frac{t}{\tau_{mol}}\right)^{x'} \quad (3)$$

where G_u is the unrelaxed modulus referred to α relaxation, A and A' are proportionality factors that depend mainly on the concentration C_d of defects, and χ' ($\chi < \chi' < 1$) is an exponent that takes into consideration the fact that segmental mobility (i.e. χ) is affected by strain above a threshold of strain. Time τ_{mol} is given by equations (1) and (2). The corresponding complex shear modulus was obtained by considering the Fourier transform of $J(t)^{-1}$ (equation (3)) such that:

$$G^*(i\omega) = G_r + \frac{G_u - G_r}{1 + (i\omega\tau_{mol})^{-\chi} + Q(i\omega\tau_{mol})^{-\chi'}} \quad (4)$$

where G_r is the relaxed modulus for the primary, or α, relaxation, which corresponds to the value of the modulus at the rubbery plateau, and Q is a constant of the order of unity. Cavaille et al.[32] have shown that these equations satisfactorily fit the data obtained for α relaxation in the case of nine different polymers including amorphous homopolymers, a random copolymer, blends and a crosslinked thermoset resin.

It is possible to fit theoretical predictions given in equation (4) to measured G' and G'' values using a Cole–Cole diagram (G_u and G_r are the high- and low-frequency limits of G', respectively; χ and χ' correspond to the slope at these limits, and Q is determined by the maximum value of G'' (ref. 33)). *Figure 4* shows a fair agreement with the parameters reported in *Table 5*. The main information is given by the χ' values. In fact, the theoretical approach given in this paper indicates that, as χ' is low, the chain segments are shorter, which is the case for DGEBA/IPD compared to DGEBA/IPD/TMCA 50/50. It is worth noting that χ is low when the number of obstacles (crosslinks) increasing the hierarchical correlation effect is maximum, i.e. for the DGEBA/IPD network. Moreover, above T_g, χ is temperature-dependent since that parameter depends on C_d; consequently, $\tau_{mol}(T)$ (see equations (1) and (2)) can be satisfactorily described by the so-called Vogel–Fulcher–Tammann (VFT) law, or similarly the Williams–Landel–Ferry (WLF) equation. In that respect, the parameter C_d has to be compared to v_F of the free-volume approach, but the description briefly recalled here applies for $T < T_g$ as well: $C_d(T_g)$, i.e. $\chi(T_g)$, is then constant, yielding a linear variation of $\log(\tau_{mol}(T))$ in an Arrhenius plot. This point, described in detail elsewhere[33], will not be developed here since we
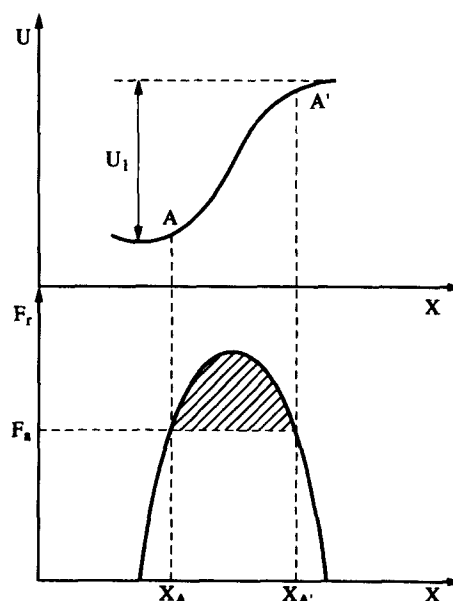
shall rather consider the response of our materials to high stresses.

So, recently, this theory was extended, using the same fundamental physical concepts in order to take into account the large-stress effects on the observed mechanical response of glassy polymers[34]. The theoretical developments have already been presented in detail[31,35,36] and will only be outlined in this article. One of the main points of this development is related to the thermo-mechanical activation of molecular motions resulting in relaxation. Beyond the details of the molecular motions involved in this relaxation, the jump between two configurations over an energy barrier of high U_1 has to be considered. At a low stress level, those jumps are only thermally activated, the energy profile being only biased. In the case of large stresses, the force F_a acting on the mobile entities is directly proportional to the stress according to $F_a = B\sigma$, where B is a proportionality constant with units of area. At equilibrium, this force is equal to the reacting force F_r of the system, which is defined as $F_r = dU/dx$.

The variations of U and F_r are schematically displayed in *Figure 5*. The coordinate x_A, representing the position corresponding to configuration A, is thus located at the first intersection between the F_r curve and the horizontal line cutting the F axis on F_a. Let us define A', i.e. the position along the x axis of the second intersection between the F_r and the F_a curves, as indicated in *Figure 5*. If the system in configuration A acquires a sufficient thermal energy to change its configuration from A to A', then the acting force F_a due to mechanical activation will ultimately drive the system over the energy barrier. In other words, the minimum thermal energy ΔH_a required to change the configuration of the system is given by the hatched area in *Figure 5*:

$$\Delta H_a = \int_{x_A}^{x_{A'}} (F_r - B\sigma)\, dx$$

In order to develop a quantitative analysis of combined mechanical and thermal energy on the

Table 5 Cole–Cole parameters for the three networks

	$G_r{}^a$ (MPa)	$G_u{}^b$ (MPa)	χ'	χ	Q
DGEBA/IPD	11	570	0.75	0.24	1
DGEBD/IPD	6	1280	0.74	0.22	1.32
DGEBA/IPD/TMCA 50/50	5	1070	0.89	0.27	1.15

a Relaxed shear modulus
b Non-relaxed shear modulus

Figure 5 Energetic considerations for determining the activation volume

mechanical response of polymers, an analytical expression for F_r is required. With a parabolic shape for the F_r function, which is usually assumed to have a sinusoidal shape, the corresponding expression giving the calculated activation enthalpy is[31]:

$$\Delta H_a = U_1 \left(1 - \frac{\sigma}{\sigma_0} \right)^{3/2}$$

which must be used instead of U_1 in equation (2). Then, the mean time corresponding to a translational degree of freedom is stress-dependent since equation (1) has to be replaced by:

$$\tau_{\text{mol}}(\sigma) = t_0 \left(\frac{\tau_1(\sigma)}{t_0} \right)^{1/\chi} \tag{5}$$

In the stationary flow regime, equation (3) can be simplified to:

$$\dot{\epsilon} \sim \tau_{\text{mol}}(\sigma)^{-1} \tag{6}$$

σ_0 is the stress that would be required to move the system over the energy barrier when no thermal energy is available (i.e. at 0 K). From Frenkel's arguments, one has $\sigma_0 \simeq G_0/2\pi$. Such a picture means that the mechanical response of a glassy polymer involves the same segmental motion as for α relaxation but at a temperature that is the lower as the stress is higher. In other words, the α mechanical relaxation is shifted towards lower temperatures when the stress is increased; as shown in another work[37], for high stresses, α processes merge with elementary molecular movements.

The activation volume related to the thermomechanical activation resulting in the elementary molecular movement is:

$$V_a = \frac{d(\Delta H_a)}{d\sigma} = \frac{3}{2} \frac{U_1}{\sigma_0} \left(1 - \frac{\sigma}{\sigma_0} \right)^{1/2} \tag{7}$$

Then, the mechanical response of glassy polymers at low temperature (i.e. high stresses) is characterized by an experimental activation volume V_{exp} obtained from equations (5) and (6) and which can be identified as V_a.

Thus, measuring U_1 by mechanical spectroscopy and G_0 by u.s. method should give $V_a(T)$ since σ_p (experimental flow shear stress) is temperature-dependent. Calculated $V_a(T/T_g)$ curves are given in *Figure 3*: those calculations are limited to the temperature range $0 < T/T_g < 0.4$ because, for higher temperature, (i) hierarchical constraints prevent us from reducing the experimental activation volume to the one corresponding to the elementary molecular movement and (ii) it has been shown[31] that, for $T/T_g > 0.5$, the microstructural state (q.p.d. concentration C_d) is temperature-dependent in the plastic flow stationary regime. This results in an apparent activation volume much higher than the true one[35]. The remarkable features exhibited in *Figure 3* are:

(i) Calculated and experimental data are in fairly good agreement.
(ii) The low V_a value for DGEBD/IPD is clearly explained considering that the elementary molecular movements concern conformational changes in CH_2 sequences ($U_1 = U_\gamma$); for other materials, $U_1 = U_\beta$ (see *Table 4*).
(iii) Calculated V_a is equal to zero when $T = 0\,K$,
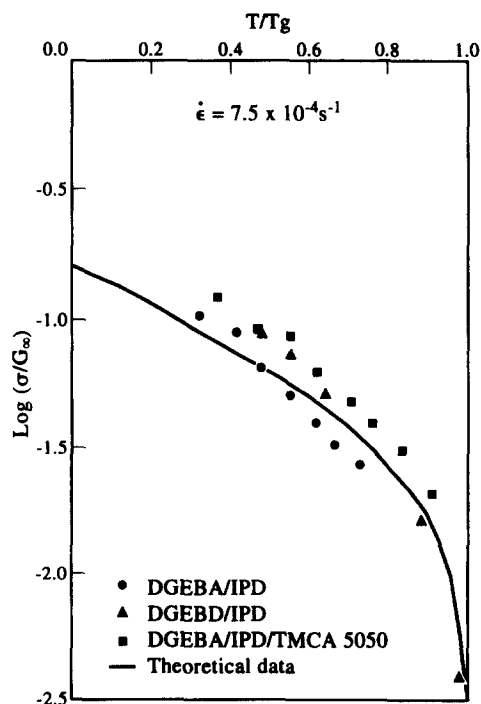

Figure 6 Global diagram with normalized axis of the mechanical properties of the three networks

which is self-consistent with the thermomechanical activation concept.

Let us consider the increase of V_{exp} with temperature at high temperatures. As previously mentioned, the main feature is the microstructural changes with temperature implying polymer self-diffusion. Then, all the constitutive parts of the repeat units need to participate in the movement and the less mobile ones need conformational change at the level of hydroxy ether groups. Consequently, the temperature ratio T_β/T_g increases from DGEBA/IPD (0.5) to DGEBA/IPD./TMCA (0.59) and DGEBD/IPD (0.61). This could explain the same order observed for the curves $V_{\text{exp}} = f(T/T_g)$ (see *Figure 3*).

The theoretical model used in this work leads to a variation of the flow stress with temperature. Using $\log(\sigma/G_\infty)$ vs. T/T_g plots results in diagrams with minor differences between various polymers[35]. Thus, our experimental results have been considered together in such a diagram (*Figure 6*) (moreover, the theoretical curve proposed in ref. 35 has also been drawn in the same diagram). Experimental and theoretical data have been presented at the same strain rate ($7.5 \times 10^{-4}\,s^{-1}$). Once again, a good agreement is observed, leading to the following conclusions:

(1) The main physical parameter determining the flow stress of polymers is the cohesion of the solid state resulting from intermolecular interactions. The modulus G_0 gives a good representation of this cohesion, which depends on the chemical nature of the repeat units.
(2) The loss of this cohesion, as the temperature increases, corresponds to the main mechanical relaxation associated with the glass transition T_g, which depends on the crosslink density, on the length of the chain segments and on the chain flexibility.

Actually, the diagram $\log(\sigma/G_\infty)$ vs. T/T_g is not strictly universal since some slight differences are expected between materials in the range $0.3 < T/T_g < 0.8$ due to different strain-rate sensitivities, that is the activation volume. The chain flexibility, which can be evaluated by studying the secondary mechanical relaxation, could determine this parameter.

As a conclusion, from experiments performed at low and high stresses, the non-elastic deformation of epoxy networks can be analysed in a coherent frame using a previously proposed molecular theory. This leads to some relations between the various experimental aspects of mechanical behaviour of the polymers to their molecular architecture.

REFERENCES

1   Gupta, V. B., Dizal, L. T. and Lee, C. Y. C. *Polym. Eng. Sci.* 1985, **25**, 812
2   Jordan, C., Galy, J. and Pascault, J. P. *J. Appl. Polym. Sci.* 1992, **46**, 859
3   Amdouni, N., Sautereau, H., Gerard, J. F. and Pascault, J. P. *Polymer* 1990, **31**, 1245
4   Ilavsky, M., Zelenka, J., Spacek, V. and Dusek, K. *Polym. Networks Blends* 1992, **2**(2), 95
5   Misra, S. C., Manson, J. A. and Sperling, L. H. *ACS Adv. Chem. Ser.* 1979, **114**, 137
6   Vaskil, U. M. and Martin, G. C. *J. Appl. Polym. Sci.* 1992, **46**, 2089
7   Charlesworth, J. M. *Polym. Eng. Sci.* 1988, **28**, 221
8   Won, Y. G., Galy, J., Gerard, J. F., Pascault, J. P., Bellenger, V. and Verdu, J. J. *Polymer* 1990, **31**, 1787
9   Halary, J. L., Cukierman, S. and Monnerie, L. *Bull. Soc. Chim. Belg.* 1989, **98**, 9
10 Urbacewski, E., Galy, J., Gerard, J. F., Pascault, J. P. and Sautereau, H. *Polym. Eng. Sci.* 1991, **31**(22), 1572
11 Choy, I. and Placek, D. *J. Polym. Sci. (B) Polym. Phys.* 1986, **24**, 1303

12 Grillet, A. C., Galy, J., Gerard, J. F. and Pascault, J. P. *Polymer* 1991, **32**(10), 1885
13 Delvigs, P. *Polym. Compos.* 1986, **7**, 101
14 Cao, Z., Galy, J., Gerard, J. F. and Sautereau, H. *Polym. Networks Blends* 1993, **4**(1), 15
15 Etienne, S., Cavaille, J. Y. and Perez, J. *Rev. Sci. Instrum.* 1992, **53**(8), 1261
16 Guiu, F. and Pratt, P. L. *Phys. Status Solidi* 1964, **6**, 111
17 Charlesworth, J. M. *Polym. Eng. Sci.* 1988, **28**(4), 229
18 Ashby, M. F. and Jones, D. R. H. 'Matériaux', Dunod, Paris, 1991, p. 49
19 Etienne, S., Guenin, G. and Perez, J. *J. Phys. (D) Appl. Phys.* 1979, **12**, 2189
20 Williams, J. G. *J. Appl. Polym. Sci.* 1979, **23**, 3433
21 Ochi, M., Shimbo, M. and Takaskima, N. *J. Polym. Sci.* 1986, **23**, 2185
22 Laupretre, F., Eustache, R. P. and Monnerie, L. *Polym. Prepr.* 1992, **33**(1), 136
23 Garton, A., McLean, P., Stevenson, W. T. K., Clark, J. N. and Daly, J. N. *Polym. Eng. Sci.* 1987, **27**, 1620
24 Bowden, P. B. and Raha, S. *Phil. Mag.* 1974, **22**, 149
25 Argon, A. S. *Phil. Mag.* 1973, **28**, 839
26 Yamini, S. and Young, R. J. *J. Mater. Sci.* 1980, **15**, 1814
27 Oleinik, E. F., Salamatina, O. B., Rudnev, S. N. and Shenogin, S. V. *Polym. Sci.* 1993, **35**(11), 1532
28 Escaig, B. *Am. Phys.* 1978, **3**, 207
29 Caux, X., Coulon, G. and Escaig, B. *Polymer* 1988, **29**, 808
30 Perez, J., Cavaille, J. Y. and Jourdan, C. *Rev. Phys. Appl.* 1988, **23**, 125
31 Perez, J. 'Physique et Mécanique des Polymères Amorphes', Tec. et Doc. Lavoisier, Paris, 1992
32 Cavaille, J. Y., Perez, J. and Johari, G. P. *J. Non-Cryst. Solids* 1989, **131–133**, 935
33 Perez, J. and Cavaille, J. Y. *J. Non-Cryst. Solids* 1994, **172–174**, 1028
34 Bouquerel, F., Bourgin, P. and Perez, J. *Polymer* 1992, **33**(3), 516
35 Mangion, M., Cavaille, J. Y. and Perez, J. *Phil. Mag. (A)* 1992, **66**(5), 773
36 Perez, J. and Lefebvre, J. 'Introduction à la Mécanique des Polymères' (Ed. C. G'sell), INPL, 1995, p. 289
37 Quinson, R., Perez, J., Germain, Y. and Murraciole, J. M. *Polymer* 1995, **36**(4), 743